

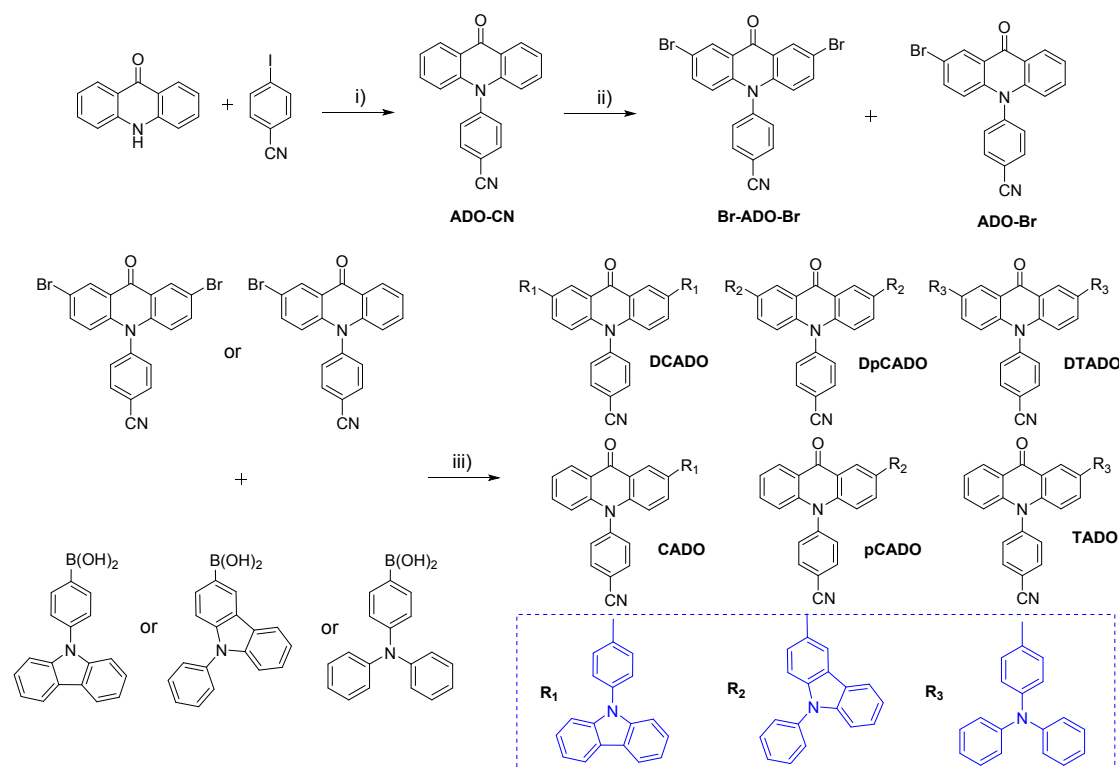
Electronic Supplementary Information (ESI)

Feasible structure-modification strategy for inhibiting aggregation-caused quenching effect and constructing exciton conversion channels in acridone-based emitters

Qing Wan,^{a#} Bing Zhang,^{a#} Jialin Tong,^c Yin Li,^a Haozhong Wu,^a Han Zhang,^a Zhiming Wang,^{a,c*} Yuyu Pan,^{c*} and Ben Zhong Tang^{a,b*}

1. General information

All the chemical agents were purchased from commercial sources and directly used without further purification. The end-products were further purified by vacuum sublimation for the investigation of photoluminescence (PL) and electroluminescence (EL) properties. ¹H and ¹³C NMR spectra were measured on a Bruker AV 500 spectrometer in CDCl₃ and CD₂Cl₂ at room temperature. UV-vis absorption spectrum was measured on a Shimadzu UV-2600 spectrophotometer. PL spectra were recorded on a Horiba Fluoromax-4 spectrofluorometer. Fluorescence quantum yields were measured using a Hamamatsu absolute PL quantum yield spectrometer C11347 Quantaurus_QY. Cyclic voltammogram was measured in a solution of tetra-n-butylammonium hexafluorophosphate (Bu₄NPF₆, 0.1 M) in dichloromethane and dimethyl formide containing the sample at a scan rate of 100 mV s⁻¹. Three-electrode system (Ag/Ag⁺, platinum wire and glassy carbon electrode as reference, counter and work electrode respectively) was used in the CV method. HOMO = -[E_{ox} + 4.8] eV, and LUMO = -[E_{re} + 4.8] eV. E_{ox} and E_{re} represent the onset oxidation and reduction potentials relative to Fe/Fe⁺. The natural transition orbitals (NTOs) were calculated using the time dependent density function theory (TD-DFT) method with b3lyp at the basis set level of 6-31g(d,p). All the calculations were performed using Gaussian09 package.



Scheme S1 Synthetic route of CADO, pCADO, TADO, DCADO, DpCADO and DTADO. Condition: i), Cul, K₃PO₄, DMF; ii) NBS, DMF; iii) Pd(PPh₃)₄, K₂CO₃, toluene/water.

2. Synthesis and Characterization

Synthesis of 4-(9-oxoacridin-10(9H)-yl)benzonitrile (ADO-CN)

The medium product 4-(9-oxoacridin-10(9H)-yl)benzonitrile was prepared by the typical Ullmann coupling reaction. To a 100 mL flask, acridone (20 mmol, 3.9 g), 4-iodobenzonitrile (25 mmol, 5.7 g), copper(I) iodide (2.5 mmol, 475 mg), K₃PO₄ (20 mmol, 4.3 g) and 2,2,6,6-tetramethylheptane-3,5-dione (5 mmol, 920 mg) were added. The air in flask contained mixtures was removed by pumping and filling in with N₂ for three times. After then, hydrous dimethyl formamide (80 mL) was injected into flask. The reaction mixture was stirred at 180 °C for 24 h. The reaction was quenched with distilled water, and extracted with dichloromethane several times. The combined organic layer was washed with distilled water for several times to remove residual dimethyl formamide, and dried with hydrous MgSO₄ for one night. After filtration and solvent evaporation under reduced pressure, the crude product was purified by column chromatography on silica gel (dichloromethane: petroleum = 1:20 v/v) to afford white powders. (yield: 56%). ¹H NMR: (500 MHz, CDCl₃): δ 8.59 (m, 2H), 8.06 (d, 2H), 7.51-7.59 (m, 4H), 7.30-7.33 (m, 2H), 6.65 (d, 2H).

Synthesis of 4-(2,7-dibromo-9-oxoacridin-10(9H)-yl)benzonitrile and 4-(2-dibromo-9-oxoacridin-10(9H)-yl)benzonitrile (Br-ADO-Br and ADO-Br)

In a dry flask, the raw material of 4-(9-oxoacridin-10(9H)-yl)benzonitrile (10 mmol, 2.96 g) in hydrous dimethyl formamide (20 mL) was put into flask. N-Bromosuccinimide (NBS, 20 mmol, 3.56 g) in hydrous dimethyl formamide (10 mL) was gradually added into flask at 0 °C in the dark. After completion of the reaction monitored by thin layer chromatography, the reaction was quenched with distilled water, and extracted with dichloromethane several times. The combined organic layer was washed with distilled water for several times to remove residual dimethyl formamide, and dried with hydrous MgSO₄ for one night. After filtration and solvent evaporation under reduced pressure, the crude product was purified by column chromatography on silica gel (dichloromethane: petroleum = 1:100 v/v) to afford white powders (4.6 g). Because of the difficult separation of 4-(2,7-dibromo-9-oxoacridin-10(9H)-yl)benzonitrile and 4-(2-dibromo-9-oxoacridin-10(9H)-yl)benzonitrile via column chromatography, these synthetic mixtures was directly used to next process.

Synthesis of 4-(2-bis(4-(diphenylamino)phenyl)-9-oxoacridin-10(9H)-yl)benzonitrile (DTADO)

The Br-ADO-Br and ADO-Br mixture (2.3 g), (4-(diphenylamino)phenyl)boronic acid (12.5 mmol, 3.6 g), Pd(PPh₃)₄ (0.1mmol, 115 mg) were put into the dry flask and pumped and filled in with N₂ for three times. The toluene (40 mL) and K₂CO₃ aqueous solution (2 M, 12 mL) were injected into the flask. After completion of the reaction monitored by thin layer chromatography, the reaction solution was extracted with dichloromethane, the organic layer was dried with hydrous MgSO₄ for one night. After filtration and solvent evaporation under reduced pressure, the crude product was purified by column chromatography on silica gel (dichloromethane: petroleum = 1:20 v/v) to afford TPA-ADO-TPA yellow powders (1.9 g). ¹H NMR (500 MHz, CDCl₃): δ 8.75 (d, 2H), 8.11 (d, 2H), 7.80 (m, 2H), 7.66 (d, 2H), 7.60 (d, 4H), 7.30 (m, 8H), 7.13-7.15 (m, 12H), 7.06-7.09 (t, 4H), 6.77 (d, 2H). ¹³C NMR (126 MHz, CDCl₃): δ 177.92, 147.57, 143.18, 141.22, 135.13, 134.63, 133.14, 132.00, 131.64, 129.34, 127.60, 124.58, 123.78, 123.12, 122.11, 116.73, 114.10. HRMS (C₅₆H₃₈N₄O): m/z 782.3046 [M⁺, calcd 782.3039].

Synthesis of 4-(2,7-bis(4-(diphenylamino)phenyl)-9-oxoacridin-10(9H)-yl)benzonitrile (TADO)

The synthetic procedure was analogous to that described for DTADO. Yellow powders of TADO (1.7 g). ¹H NMR (500 MHz, CDCl₃): δ 8.79(d, 1H), 8.61 (d, 1H), 8.08 (d, 2H), 7.76 (m, 1H), 7.61-7.50 (m, 5H), 7.30-7.25 (m, 5H), 7.18-7.10 (m, 6H), 7.06-7.02 (m, 2H), 6.71 (d, 1H), 6.65 (d, 1H). ¹³C NMR (126 MHz, CDCl₃): δ 177.92, 147.57, 143.17, 141.22, 135.12, 134.63, 133.14, 132.00, 131.64, 129.34, 127.60, 124.75, 124.58, 123.77, 123.12, 122.10, 116.73, 114.10. HRMS (C₃₈H₂₅N₃O): m/z 539.1998 [M⁺, calcd 539.2059].

Synthesis of 4-(9-oxo-2-bis(9-phenyl-9H-carbazol-3-yl)acridin-10(9H)-yl)benzonitrile (DpCADO)

The synthetic procedure was analogous to that described for DTADO. Yellow powders of DpCADO (1.8 g) were obtained. ¹H NMR (500 MHz, CDCl₃): δ 9.01 (d, 2H), 8.49 (d, 2H), 8.23 (d, 2H), 8.11 (d, 2H), 7.96 (d, 2H), 7.76 (d, 2H), 7.68 (d, 2H), 7.65-7.60 (m, 8H), 7.51 (d, 4H), 7.44 (d, 4H), 7.34 (m, 2H), 6.81 (d, 2H). ¹³C NMR (126 MHz, CDCl₃): δ 178.23, 141.43, 141.19, 140.51, 137.59, 135.97, 135.15, 132.78, 131.71, 131.65, 129.97, 127.62, 127.10, 126.29, 125.24, 124.09, 123.41, 122.23, 120.50, 120.24, 118.78, 116.82, 114.10, 110.27, 109.99. HRMS (C₅₆H₃₄N₄O): m/z 778.2733 [M⁺, calcd 778.2728].

Synthesis of 4-(9-oxo-2,7-bis(9-phenyl-9H-carbazol-3-yl)acridin-10(9H)-yl)benzonitrile (pCADO)

The synthetic procedure was analogous to that described for DTADO. Yellow powders of pCADO (1.6 g) were obtained. ¹H NMR (500 MHz, CDCl₃): δ 8.94 (d, 1H), 8.64 (d, 1H), 8.46 (d, 1H), 8.22 (d, 1H), 8.09 (d, 2H), 7.92 (d, 1H), 7.74 (d, 1H), 7.65-7.58 (m, 6H), 7.54 (m, 1H), 7.48 (m, 2H), 7.44 (m, 2H), 7.34 (m, 2H), 6.77 (d, 1H), 6.69 (d, 1H). ¹³C NMR (126 MHz, CDCl₃): δ 178.07, 143.25, 142.35, 141.41, 141.29, 140.49, 137.56, 135.93, 135.13, 133.63,

132.76, 131.69, 131.56, 129.96, 127.80, 127.61, 127.08, 126.28, 125.17, 125.09, 124.08, 123.39, 122.21, 122.13, 121.89, 120.47, 120.23, 118.74, 117.67, 116.78, 116.11, 114.06, 110.25, 109.98. HRMS ($C_{38}H_{23}N_3O$): m/z 537.1841 [M $^+$, calcd 537.1851].

Synthesis of 4-(2-bis(4-(9H-carbazol-9-yl)phenyl)-9-oxoacridin-10(9H)-yl)benzonitrile (DCADO)

The synthetic procedure was analogous to that described for DTADO. Yellow powders of DCADO (1.6 g) were obtained. 1H NMR (500 MHz, $CDCl_3$): δ 8.99 (d, 2H), 8.18-8.13 (m, 6H), 7.96-7.91 (m, 6H), 7.71-7.69 (m, 6H), 7.49 (d, 4H), 7.46-7.43 (m, 4H), 7.33-7.30 (m, 4H), 6.86 (d, 2H). ^{13}C NMR (126 MHz, $CDCl_3$): δ 177.92, 142.98, 141.82, 140.79, 138.41, 137.23, 135.28, 134.31, 132.42, 131.60, 128.36, 126.03, 125.68, 123.50, 122.27, 120.37, 120.09, 117.10, 114.36, 109.82. HRMS ($C_{56}H_{34}N_4O$): m/z 778.2733 [M $^+$, calcd 778.2723].

Synthesis of 4-(2,7-bis(4-(9H-carbazol-9-yl)phenyl)-9-oxoacridin-10(9H)-yl)benzonitrile (CADO)

The synthetic procedure was analogous to that described for DTADO. Yellow powders of CADO (1.2 g) were obtained. 1H NMR (500 MHz, $CDCl_3$): δ 8.89 (d, 1H), 8.59 (d, 1H), 8.10 (m, 2H), 8.03 (d, 2H), 7.86 (d, 2H), 7.82 (d, 1H), 7.62 (d, 2H), 7.57 (d, 2H), 7.50 (m, 1H), 7.43 (d, 2H), 7.38-7.29 (m, 4H), 7.22 (m, 2H), 6.98 (d, 1H), 6.72 (d, 1H), 6.61 (d, 1H). ^{13}C NMR (126 MHz, $CDCl_3$): δ 177.91, 143.07, 142.39, 141.89, 140.77, 138.46, 137.13, 135.19, 134.01, 132.25, 131.63, 128.30, 127.78, 127.48, 126.01, 125.53, 123.47, 122.36, 122.17, 121.96, 120.35, 120.06, 117.61, 116.98, 116.20, 114.18, 109.81. HRMS ($C_{38}H_{23}N_3O$): m/z 537.1841 [M $^+$, calcd 537.1868].

Fabrication of OLED devices

Glass substrates pre-coated with a 95-nm-thin layer of indium tin oxide (ITO) with a sheet resistance of $20\ \Omega$ per square were thoroughly cleaned for 10 minutes in ultrasonic bath of acetone, isopropyl alcohol, detergent, deionized water, and isopropyl alcohol and then treated with O_2 plasma for 5 min in sequence. Organic layers were deposited onto the ITO-coated substrates by high-vacuum ($< 5 \times 10^{-4}$ Pa) thermal evaporation. Deposition rates were controlled by independent quartz crystal oscillators, which were $1\text{--}2\ \text{\AA s}^{-1}$ for organic materials, $0.1\ \text{\AA s}^{-1}$ for LiF, and $3\text{--}6\ \text{\AA s}^{-1}$ for Al, respectively. The emission area of the devices was $3 \times 3\ \text{mm}^{-2}$ as shaped by the overlapping area of the anode and cathode. All the device characterization steps were carried out at room temperature under ambient laboratory conditions without encapsulation except spectrum collection process. EL spectra were taken by an optical analyzer, Photo Research PR745. Current density and luminance versus driving voltage characteristics were measured by Keithley 2420 and Konica Minolta chromameter Keithley2450, respectively. External quantum efficiencies were calculated by assuming that the devices were Lambertian light sources.

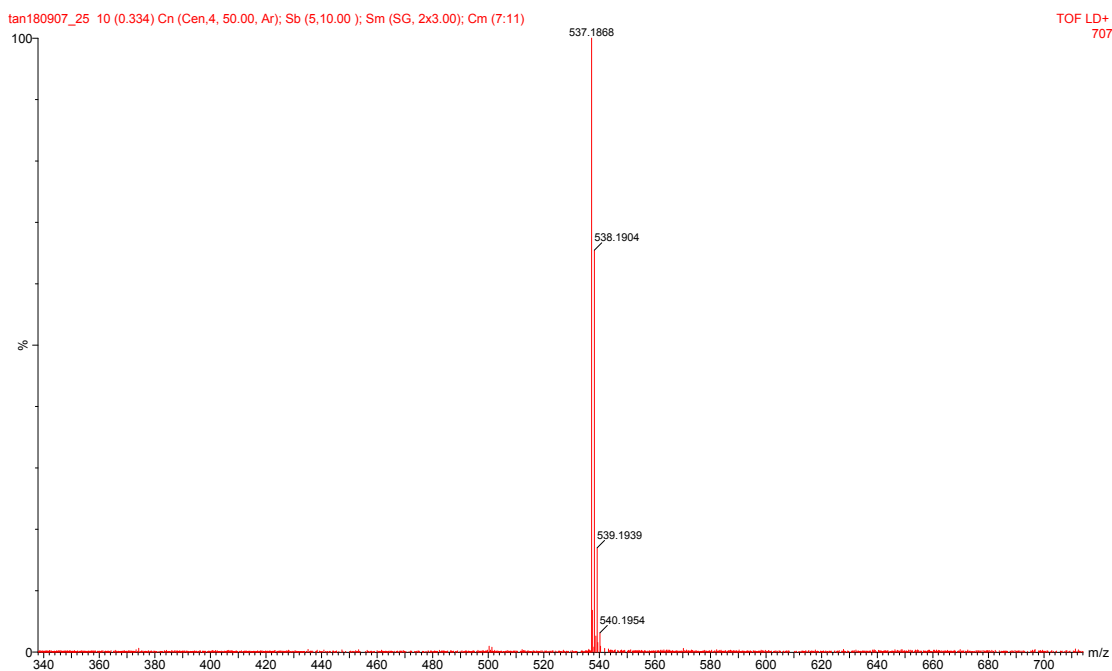


Fig. S1 The time of flight mass spectrum of CADO.

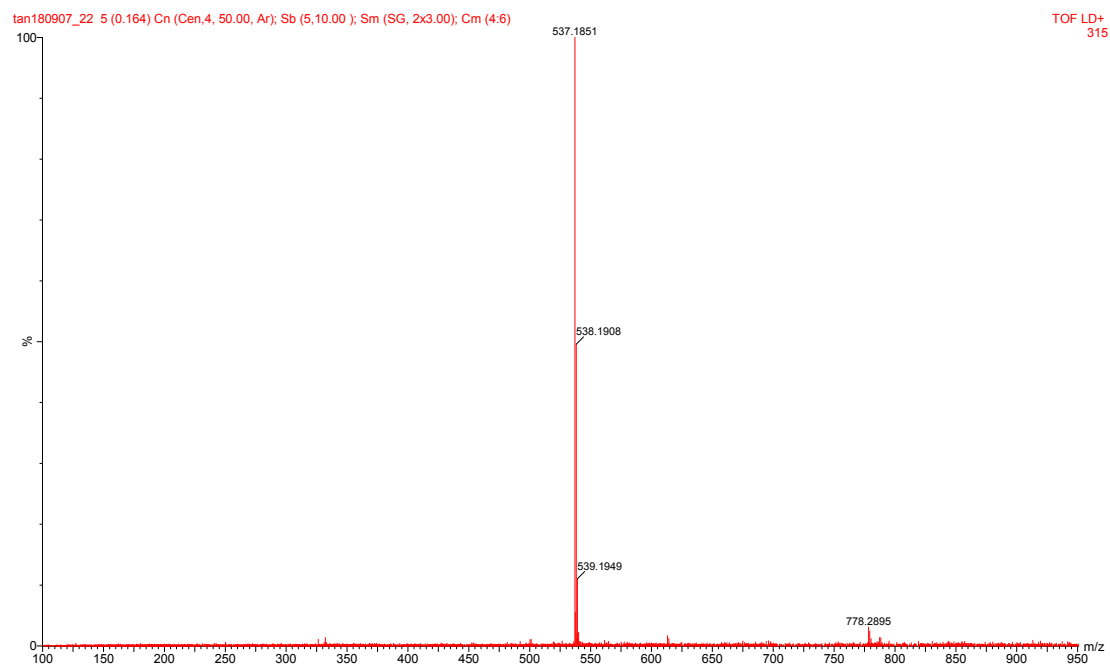


Fig. S2 The time of flight mass spectrum of pCADO.

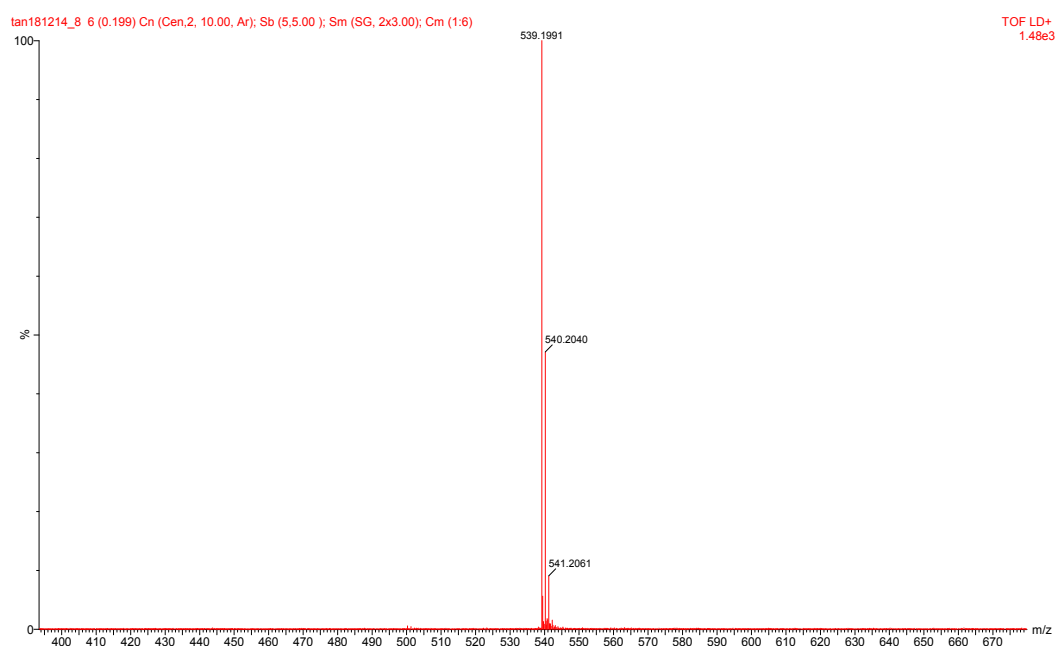


Fig. S3 The time of flight mass spectrum of TADO.



Fig. S4 The time of flight mass spectrum of DCADO.

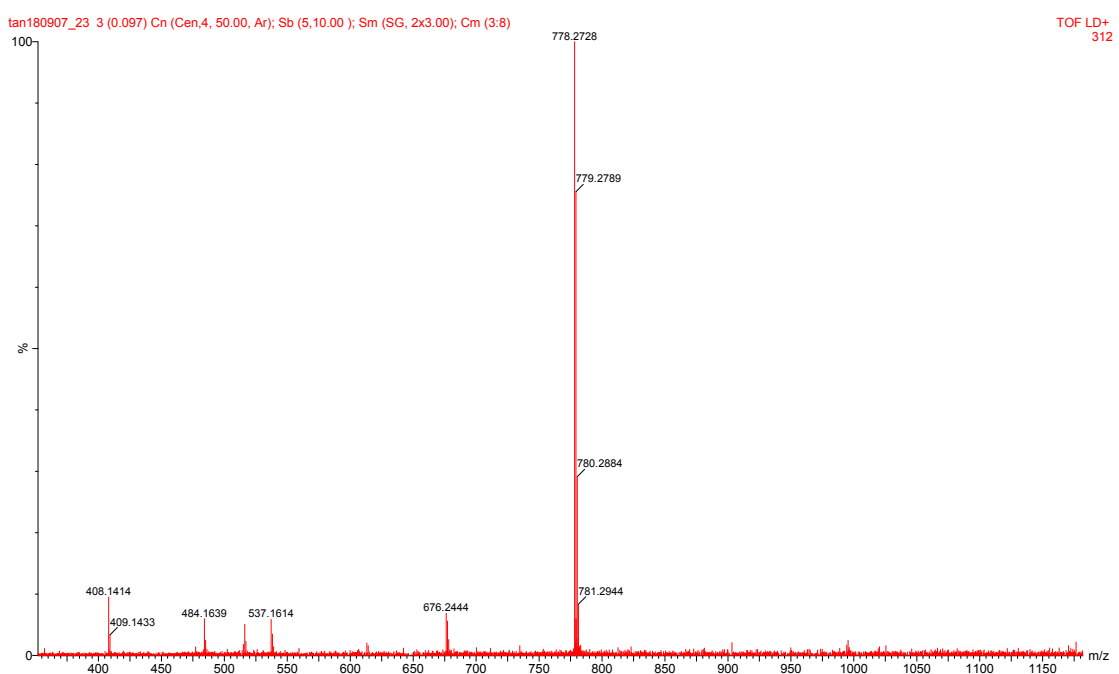


Fig. S5 The time of flight mass spectrum of DpCADO.

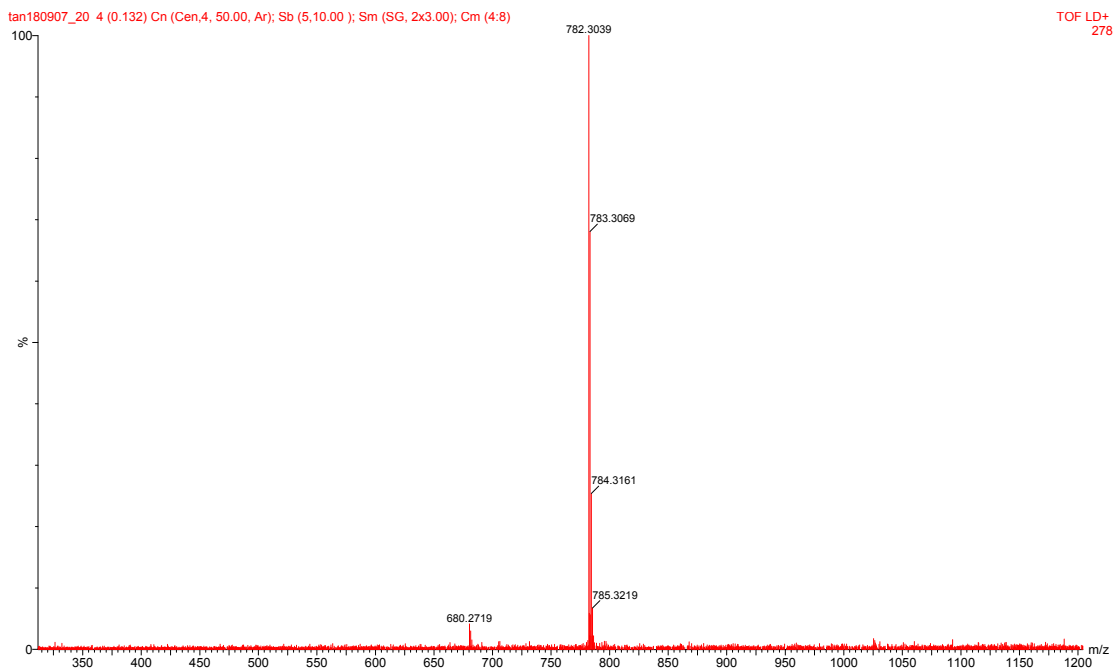


Fig. S6 The time of flight mass spectrum of DTADO.

Electron-donating ability

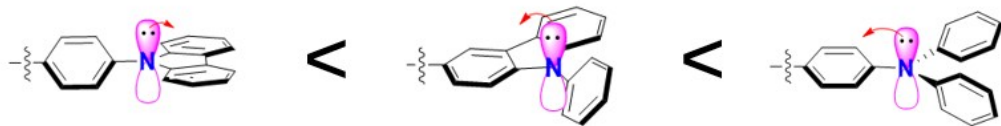


Fig. S7 The order of electron-donating ability for Cz, *p*-Cz and TPA groups.

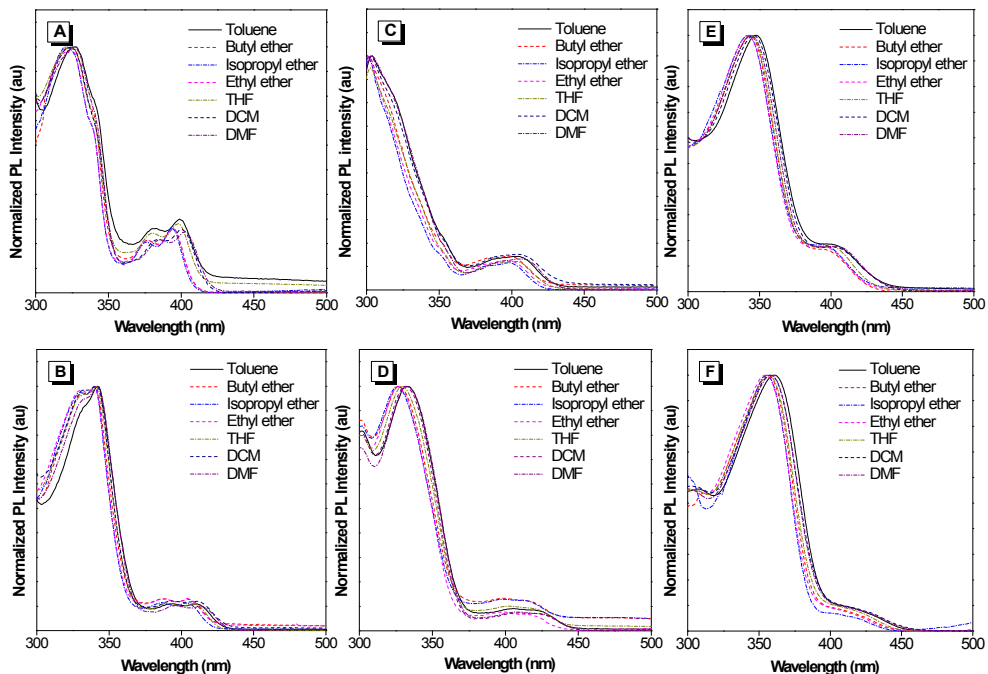


Fig. S8 UV-vis spectra of ADO-based fluorogens in different solvents with different polarity: (A) CADO, (B) DCADO, (C) *p*CADO, (D) DpCADO, (E) DTADO and (F) TADO (Concentration: 10^{-5} M).

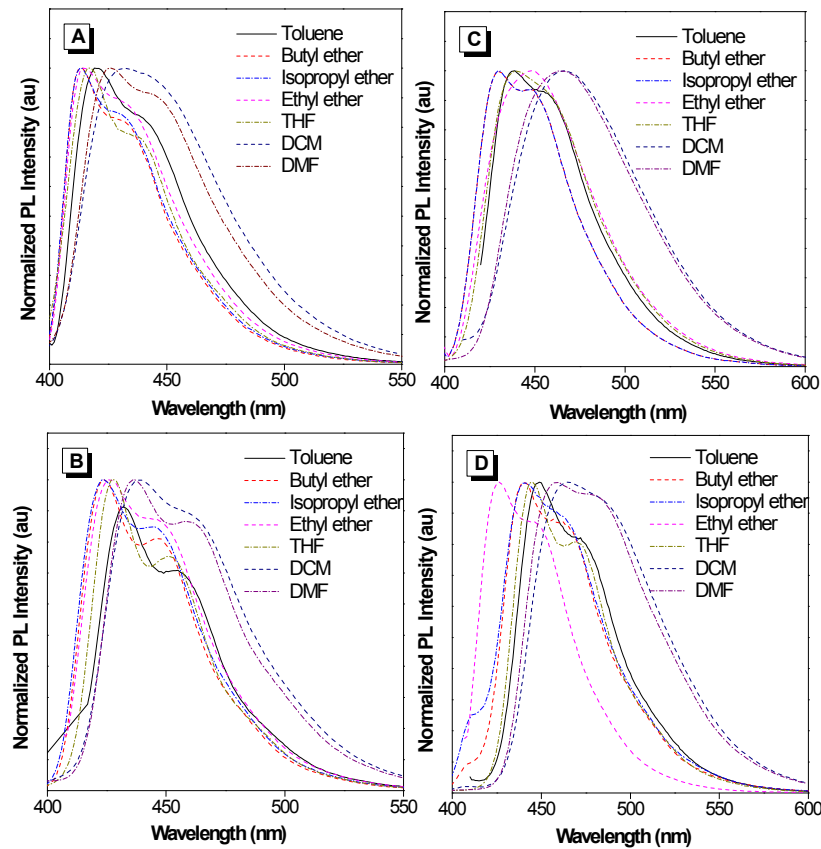


Fig. S9 PL spectra of ADO-based fluorogens in different solvents with different polarity: (A) CADO, (B) DCADO, (C) pCADO, (D) DpCADO (Concentration: 10^{-5} M).

Table S1 Detail basic photophysical data of CADO.

Solvents	ϵ	n	$f(\epsilon, n)$	λ_a (nm)	λ_f (nm)	$V_a - V_f$ (cm ⁻¹)	Φ_F (%)	Lifetime (ns)
Toluene	2.38	1.494	0.014	398	420	1316	3.6	1.70
Butyl ether	3.08	1.399	0.096	394	414	1226	4.3	1.10
Isopropyl ether	3.88	1.368	0.145	393	414	1290	4.7	1.19
Ethyl ether	4.34	1.352	0.167	395	414	1161	5.8	1.53
THF	7.58	1.407	0.210	398	428	1761	7.8	1.58
DCM	8.93	1.424	0.217	400	432	1851	15.2	2.57
DMF	37	1.427	0.276	403	426	1339	14.6	4.19

Table S2 Detail basic photophysical data of pCADO.

Solvents	ϵ	n	$f(\epsilon, n)$	λ_a (nm)	λ_f (nm)	$V_a - V_f$ (cm ⁻¹)	Φ_F (%)	Lifetime (ns)
Toluene	2.38	1.494	0.014	402	420	1939	7.8	2.98
Butyl ether	3.08	1.399	0.096	398	437	2242	9.0	2.09
Isopropyl ether	3.88	1.368	0.145	397	444	2666	9.9	2.62
Ethyl ether	4.34	1.352	0.167	399	448	2741	11.8	3.57
THF	7.58	1.407	0.210	402	444	2353	12.8	3.16
DCM	8.93	1.424	0.217	404	467	3339	26.3	6.80
DMF	37	1.427	0.276	406	466	3171	24.4	6.40

Table S3 Detail basic photophysical data of TADO.

Solvents	ϵ	n	f(ϵ, n)	λ_a (nm)	λ_f (nm)	$V_a - V_f$ (cm ⁻¹)	Φ_F (%)	Lifetime (ns)
Toluene	2.38	1.494	0.014	402	477	3911	15.2	3.98
Butyl ether	3.08	1.399	0.096	399	478	4142	12	3.11
Isopropyl ether	3.88	1.368	0.145	393	470	4169	11.5	3.67
Ethyl ether	4.34	1.352	0.167	394	470	4104	13	4.07
THF	7.58	1.407	0.210	399	482	4316	16.8	4.90
DCM	8.93	1.424	0.217	401	530	6070	29.5	12.58
DMF	37	1.427	0.276	403	541	6330	17.2	8.81

Table S4 Detail basic photophysical data of DCADO.

Solvents	ϵ	n	f(ϵ, n)	λ_a (nm)	λ_f (nm)	$V_a - V_f$ (cm ⁻¹)	Φ_F (%)	Lifetime (ns)
Toluene	2.38	1.494	0.014	412	432	1123	7.7	1.95
Butyl ether	3.08	1.399	0.096	405	442	994	6.8	1.65
Isopropyl ether	3.88	1.368	0.145	404	423	1111	6.8	1.59
Ethyl ether	4.34	1.352	0.167	404	426	1278	7.1	1.83
THF	7.58	1.407	0.210	408	428	1145	7.4	1.71
DCM	8.93	1.424	0.217	410	439	1611	12.2	2.50
DMF	37	1.427	0.276	412	437	1388	11.3	2.50

Table S5 Detail basic photophysical data of DpCADO.

Solvents	ϵ	n	f(ϵ, n)	λ_a (nm)	λ_f (nm)	$V_a - V_f$ (cm ⁻¹)	Φ_F (%)	Lifetime (ns)
Toluene	2.38	1.494	0.014	406	441	2369	11.0	3.69
Butyl ether	3.08	1.399	0.096	403	440	2086	9.5	1.50
Isopropyl ether	3.88	1.368	0.145	405	441	2015	8.7	2.76
Ethyl ether	4.34	1.352	0.167	403	448	2492	11.9	1.83
THF	7.58	1.407	0.210	402	445	2404	11.1	3.24
DCM	8.93	1.424	0.217	417	465	2475	25.9	7.39
DMF	37	1.427	0.276	406	458	2796	22.4	6.14

Table S6 Detail basic photophysical data of DTADO.

Solvents	ϵ	n	f(ϵ, n)	λ_a (nm)	λ_f (nm)	$V_a - V_f$ (cm ⁻¹)	Φ_F (%)	Lifetime (ns)
Toluene	2.38	1.494	0.014	413	467	2799	11.3	3.38
Butyl ether	3.08	1.399	0.096	409	478	3529	8.9	2.97
Isopropyl ether	3.88	1.368	0.145	403	477	3849	8.9	3.28
Ethyl ether	4.34	1.352	0.167	410	480	3557	9.8	3.57
THF	7.58	1.407	0.210	399	493	4779	13.9	4.76
DCM	8.93	1.424	0.217	399	530	6194	27.5	12.03
DMF	37	1.427	0.276	416	544	5656	17.6	8.99

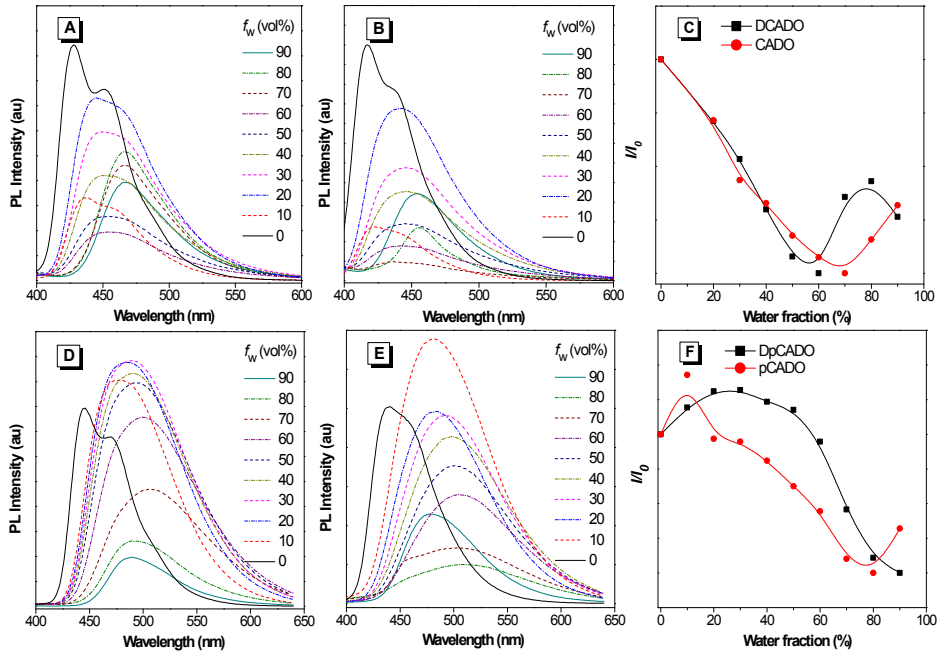


Fig. S10 PL spectra of ADO-based fluorogens in THF/water mixtures with different water fraction: (A) DCADO, (B) CADO, (C) Plots of I/I_0 versus water fractions in THF-water mixtures, (D) DpCADO and (E) pCADO and (F) Plots of I/I_0 versus water fractions in THF-water mixtures. Where I_0 is the PL intensity in pure THF solution. (Concentration: 10^{-5} M).

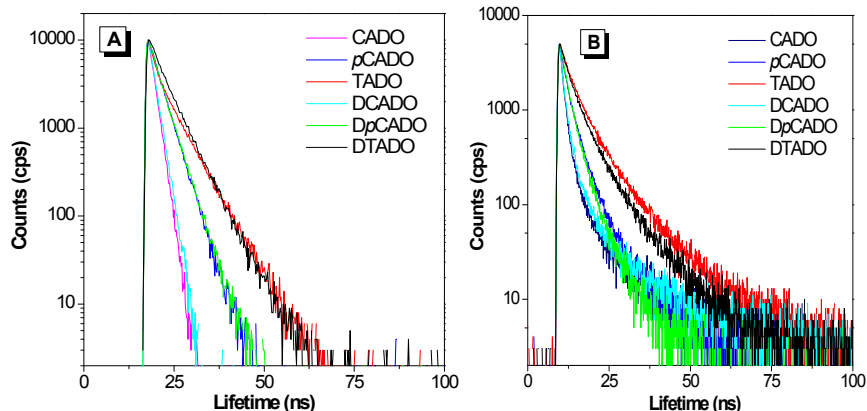


Fig. S11 Transient PL delay behavior of six ADOs under the (A) THF solution (Concentration: 10^{-5} M), (B) neat film (60 nm).

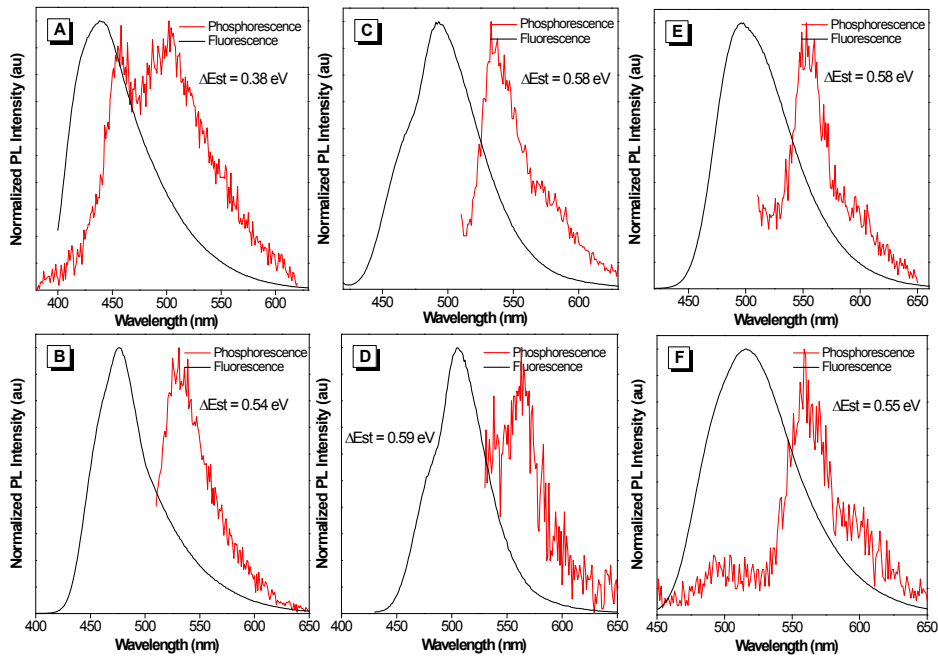


Fig. S12 Fluorescence and phosphorescence spectra of (A) CADO, (B) DCADO, (C) *p*CADO, (D) *Dp*CADO, (E) TADO and (F) DTADO, measured at 77 K.

Table S7 NTOs distribution and clear information of S_1 - S_{10} of CADO.

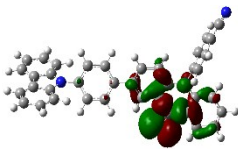
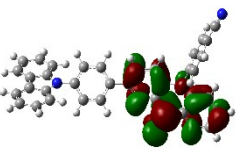
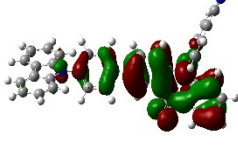
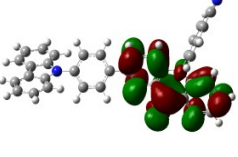
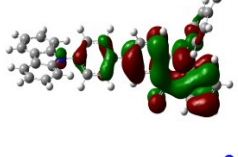
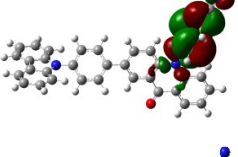
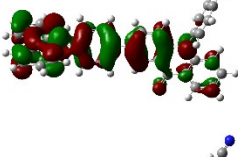
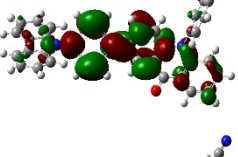
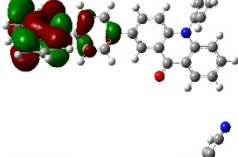
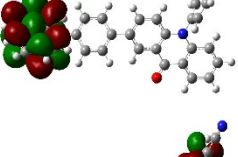
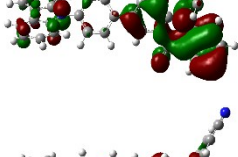
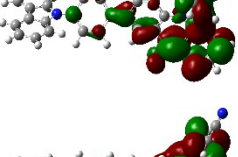
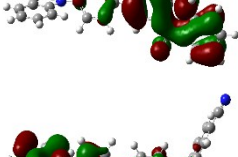
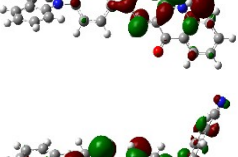
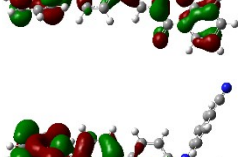
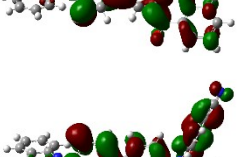
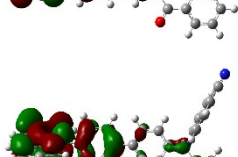
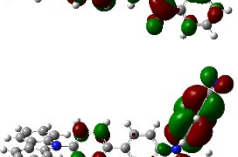
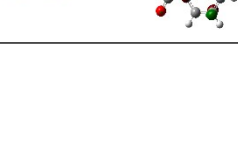
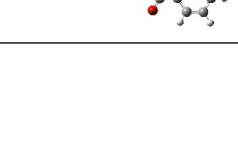
State	Hole	Particle	Oscillator strength	Transition character	Energy Level (EV)
S_1			0.0107	LE	3.78
S_2			0.0933	HLCT	3.81
S_3			0.0005	CT	3.87
S_4			1.0060	LE	4.18
S_5			0.0283	LE	4.31
S_6			0.0462	HLCT	4.43
S_7			0.0126	HLCT	4.62
S_8			0.0682	HLCT	4.69
S_9			0.0392	HLCT	4.74
S_{10}			0.0048	CT	4.75

Table S8 NTOs distribution and clear information of T₁-T₁₀ of CADO.

State	Hole	Particle	Oscillator strength	Transition character	Energy Level (EV)
T ₁			-	HLCT	2.95
T ₂			-	LE	3.41
T ₃			-	LE	3.44
T ₄			-	LE	3.62
T ₅			-	LE	3.67
T ₆			-	LE	3.79
T ₇			-	HLCT	3.85
T ₈			-	HLCT	3.87
T ₉			-	LE	3.94
T ₁₀			-	HLCT	4.02

Table S9 NTOs distribution and clear information of S_1 - S_{10} of *p*CADO.

State	Hole	Particle	Oscillator strength	Transition character	Energy Level (EV)
S_1			0.0866	HLCT	3.73
S_2			0.0003	CT	3.76
S_3			0.0056	LE	3.79
S_4			0.0932	LE	4.15
S_5			0.5782	HLCT	4.29
S_6			0.5823	HLCT	4.44
S_7			0.0441	HLCT	4.59
S_8			0.4051	LE	4.68
S_9			0.1142	LE	4.71
S_{10}			0.0014	CT	4.78

Table S10 NTOs distribution and clear information of T₁-T₁₀ of *p*CADO.

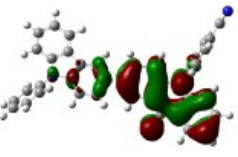
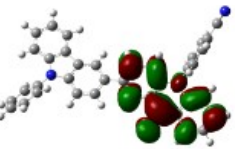
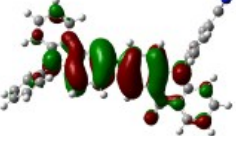
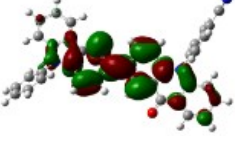
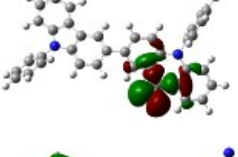
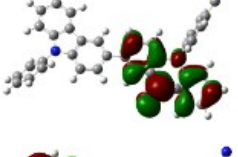
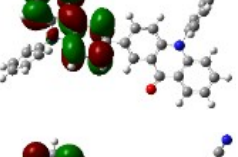
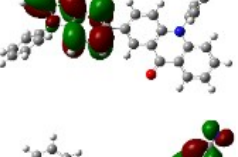
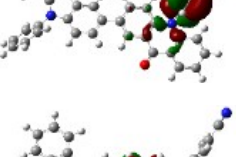
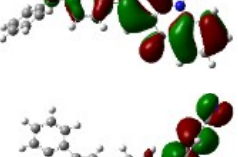
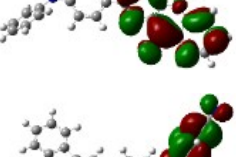
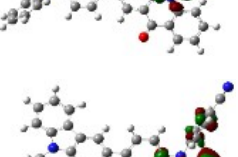
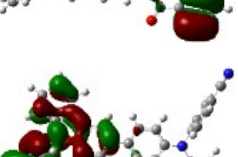
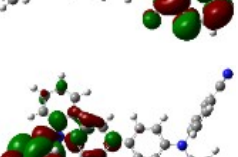
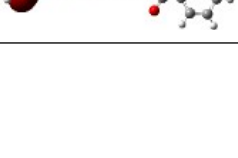
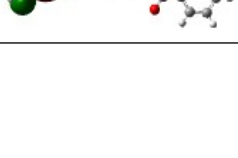
State	Hole	Particle	Oscillator strength	Transition character	Energy Level (EV)
T ₁			-	HLCT	2.91
T ₂			-	LE	3.43
T ₃			-	LE	3.45
T ₄			-	LE	3.55
T ₅			-	LE	3.70
T ₆			-	CT	3.76
T ₇			-	HLCT	3.77
T ₈			-	LE	3.85
T ₉			-	LE	3.97
T ₁₀			-	LE	3.98

Table S11 NTOs distribution and clear information of S_1 - S_{10} of TADO.

State	Hole	Particle	Oscillator strength	Transition character	Energy Level (EV)
S_1			0.0794	HLCT	3.68
S_2			0.0014	CT	3.75
S_3			0.0024	LE	3.77
S_4			1.0046	LE	3.91
S_5			0.0376	LE	4.10
S_6			0.0459	HLCT	4.28
S_7			0.2281	LE	4.32
S_8			0.0058	CT	4.45
S_9			0.0005	CT	4.50
S_{10}			0.0987	LE	4.67

Table S12 NTOs distribution and clear information of T₁-T₁₀ of TADO.

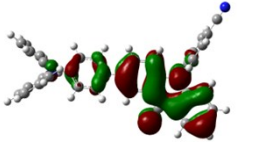
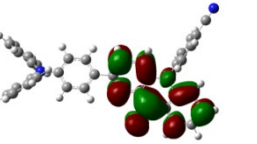
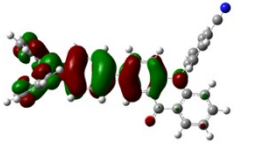
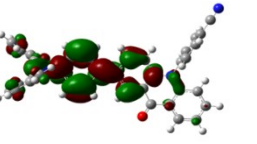
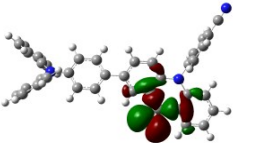
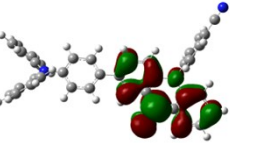
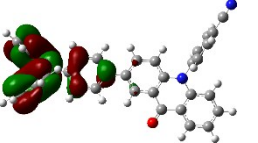
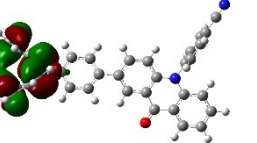
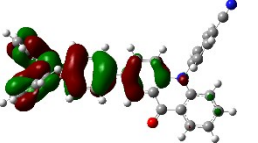
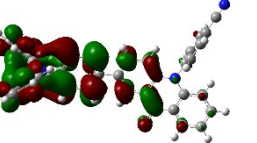
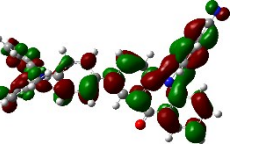
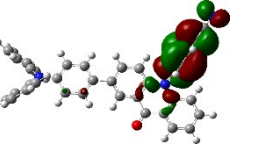
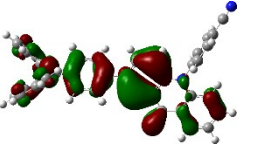
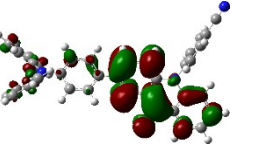
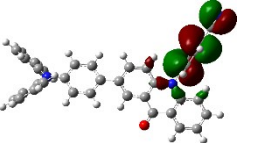
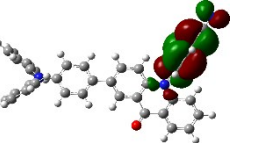
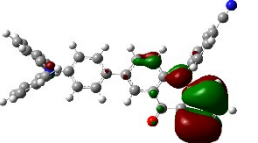
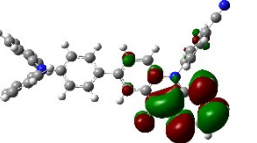
State	Hole	Particle	Oscillator strength	Transition character	Energy Level (EV)
T ₁			-	HLCT	2.91
T ₂			-	LE	3.17
T ₃			-	LE	3.45
T ₄			-	LE	3.55
T ₅			-	LE	3.70
T ₆			-	HLCT	3.74
T ₇			-	CT	3.75
T ₈			-	HLCT	3.78
T ₉			-	LE	3.85
T ₁₀			-	LE	3.96

Table S13 NTOs distribution and clear information of S_1 - S_{10} of DCADO.

State	Hole	Particle	Oscillator strength	Transition character	Energy Level (EV)
S_1			0.0686	HLCT	3.69
S_2			0.0023	LE	3.78
S_3			0	CT	3.82
S_4			1.6403	HLCT	4.02
S_5			0.1280	HLCT	4.26
S_6			0.3305	HLCT	4.29
S_7			0.0515	LE	4.31
S_8			0.0089	LE	4.31
S_9			0.0081	HLCT	4.52
S_{10}			0.0046	CT	4.60

Table S14 NTOs distribution and clear information of T₁-T₁₀ of DCADO.

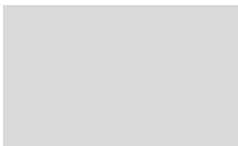
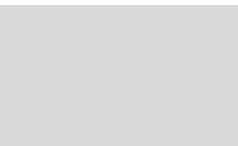
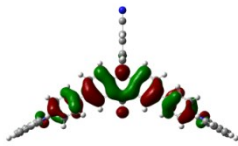
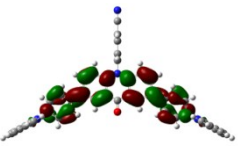
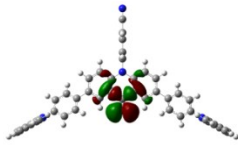
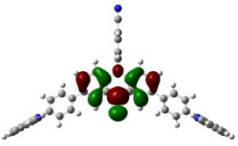
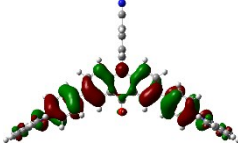
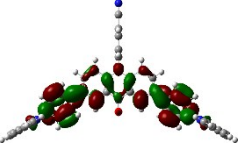
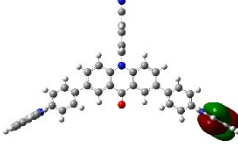
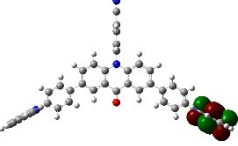
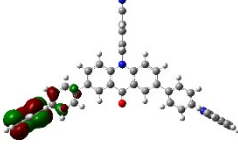
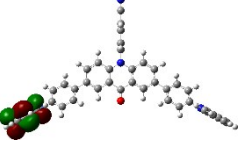
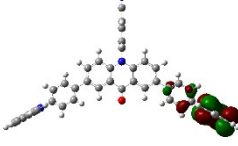
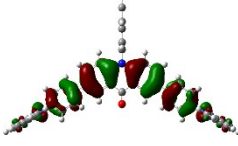
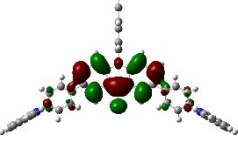
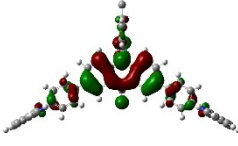
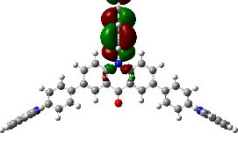
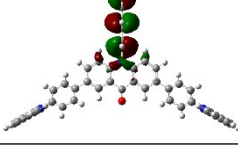
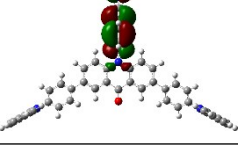
State	Hole	Particle	Oscillator strength	Transition character	Energy Level (EV)
T ₁			-	HLCT	2.88
T ₂			-	LE	3.32
T ₃			-	LE	3.44
T ₄			-	LE	3.48
T ₅			-	LE	3.62
T ₆			-	LE	3.67
T ₇			-	LE	3.67
T ₈			-	HLCT	3.80
T ₉			-	CT	3.81
T ₁₀			-	LE	3.86

Table S15 NTOs distribution and clear information of S_1 - S_{10} of DpCADO.

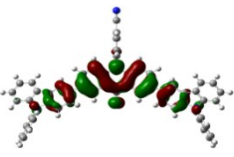
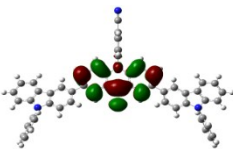
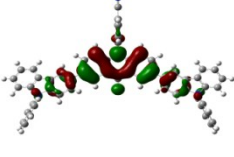
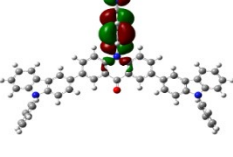
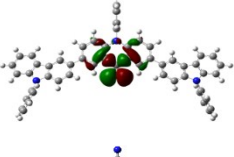
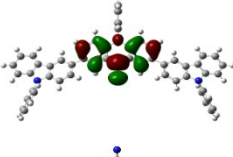
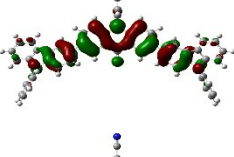
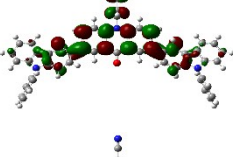
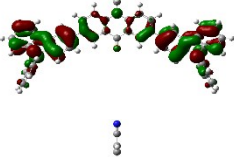
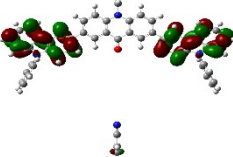
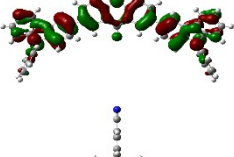
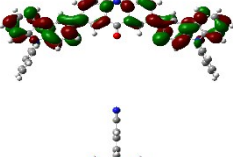
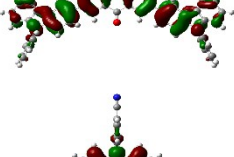
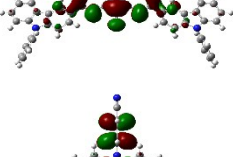
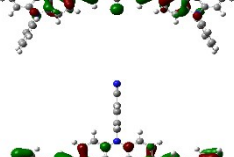
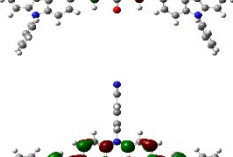
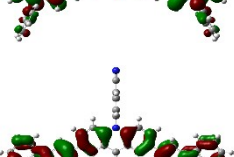
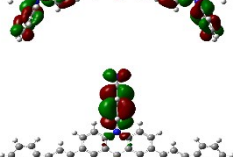
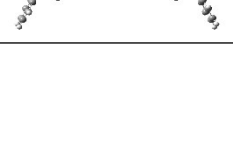
State	Hole	Particle	Oscillator strength	Transition character	Energy Level (EV)
S_1			0.0008	HLCT	3.72
S_2			0.0553	CT	3.74
S_3			0.0183	LE	3.79
S_4			1.0861	HLCT	4.15
S_5			0.0493	LE	4.28
S_6			0.4640	LE	4.29
S_7			0.7180	LE	4.38
S_8			0.0048	CT	4.57
S_9			0.4221	LE	4.66
S_{10}			0.0003	CT	4.68

Table S16 NTOs distribution and clear information of T₁-T₁₀ of DpCADO.

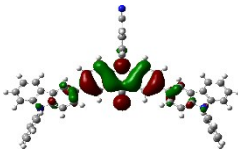
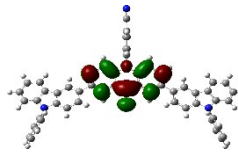
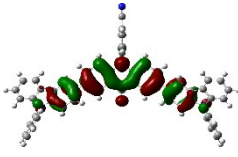
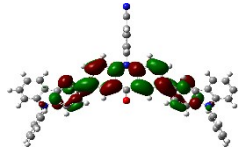
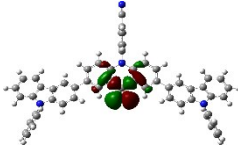
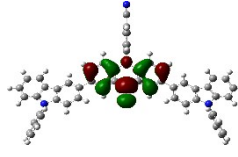
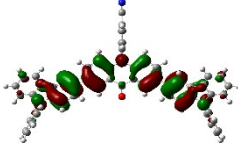
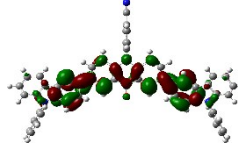
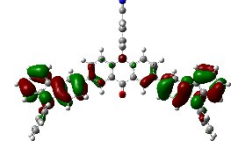
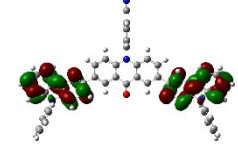
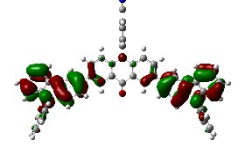
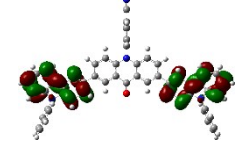
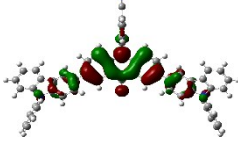
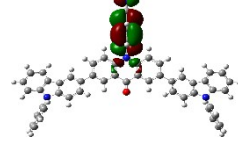
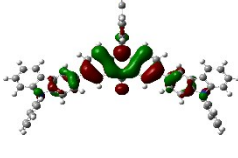
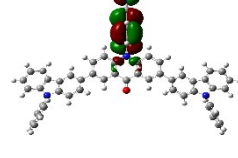
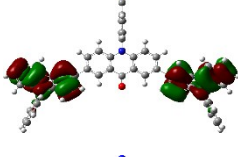
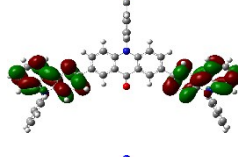
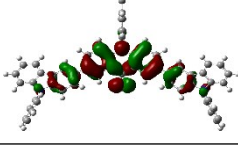
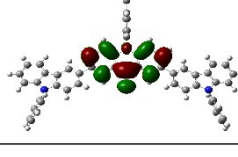
State	Hole	Particle	Oscillator strength	Transition character	Energy Level (EV)
T ₁			-	HLCT	2.91
T ₂			-	LE	3.41
T ₃			-	LE	3.42
T ₄			-	LE	3.55
T ₅			-	LE	3.63
T ₆			-	LE	3.63
T ₇			-	CT	3.72
T ₈			-	CT	3.74
T ₉			-	LE	3.79
T ₁₀			-	LE	3.84

Table S17 NTOs distribution and clear information of S_1 - S_{10} of DTADO.

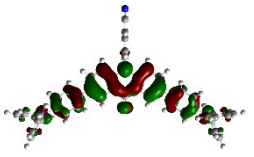
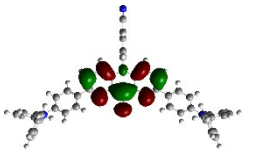
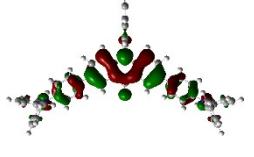
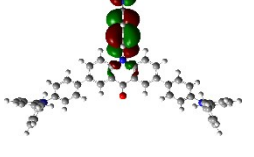
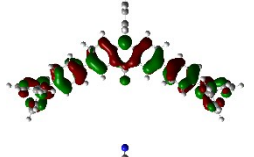
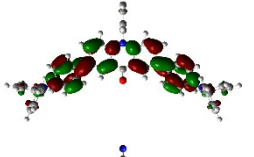
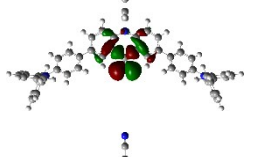
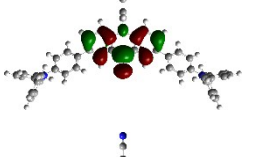
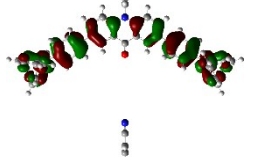
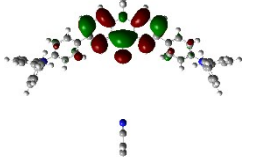
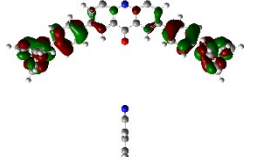
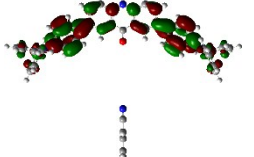
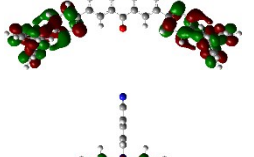
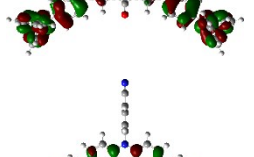
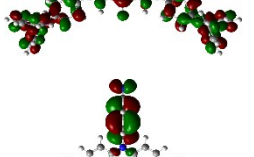
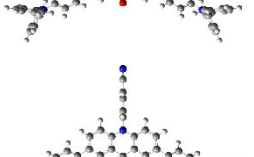
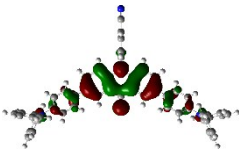
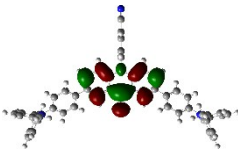
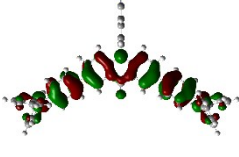
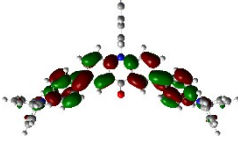
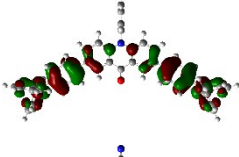
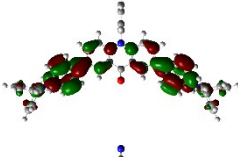
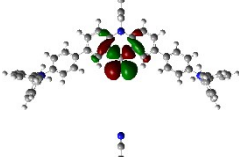
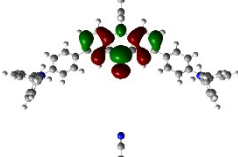
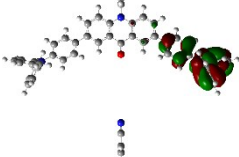
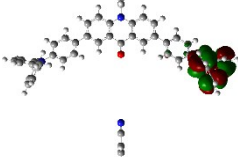
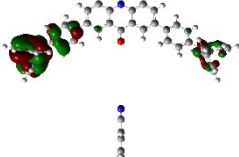
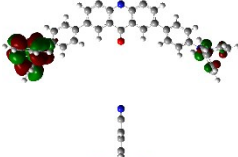
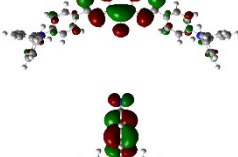
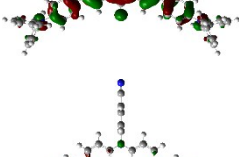
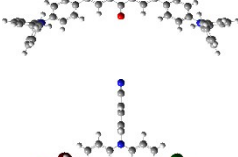
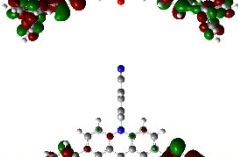
State	Hole	Particle	Oscillator strength	Transition character	Energy Level (EV)
S_1			0.0423	HLCT	2.56
S_2			0.0001	CT	3.64
S_3			1.7909	LE	3.20
S_4			0.0007	LE	3.79
S_5			0.0180	HLCT	3.97
S_6			0.3940	HLCT	4.00
S_7			0.0459	LE	4.10
S_8			0.0221	HLCT	4.11
S_9			0.0000	CT	4.28
S_{10}			0.0261	LE	4.32

Table S18 NTOs distribution and clear information of T₁-T₁₀ of DTADO.

State	Hole	Particle	Oscillator strength	Transition character	Energy Level (EV)
T ₁			-	HLCT	2.82
T ₂			-	HLCT	3.12
T ₃			-	LE	3.20
T ₄			-	LE	3.45
T ₅			-	LE	3.55
T ₆			-	LE	3.55
T ₇			-	HLCT	3.61
T ₈			-	CT	3.63
T ₉			-	LE	3.72
T ₁₀			-	LE	3.72

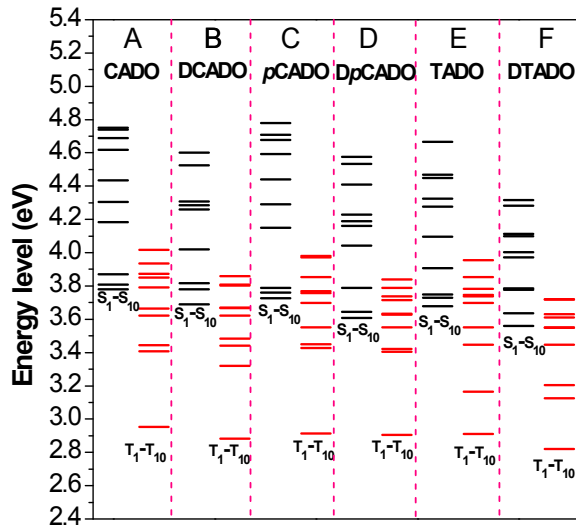


Fig. S13 The calculated Energy levels distribution of six ADO-based fluorogens.

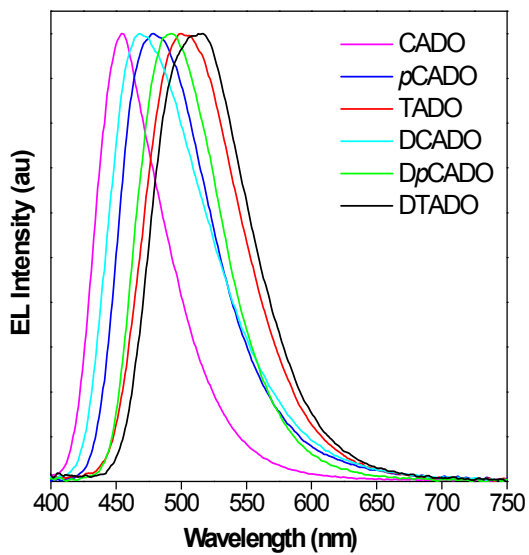


Figure S14 EL spectra of undoped OLED devices using these ADOs as lighting layer.